Molecular dynamics simulations of polyamidoamine dendrimers and their complexes with linear poly(ethylene oxide) at different pH conditions: static properties and hydrogen bonding†

I. Tanis and K. Karatasos*

Received 13th July 2009, Accepted 25th August 2009
First published as an Advance Article on the web 11th September 2009
DOI: 10.1039/b913986a

Models consisting of an amine-terminated poly(amidoamine) (PAMAM) dendrimer with and without the presence of a linear poly(ethylene oxide) (PEO) chain were studied in aqueous solutions by means of fully atomistic molecular dynamics simulations. Dendrimers of two generations, 3rd and 4th and at different pH conditions were examined, in order to address issues associated with characteristics pertinent to the shape of the dendrimers in the presence or absence of PEO as well as to the volume fraction of the penetrating solvent molecules and counterions as compared to recent experimental studies. In addition, hydrogen-bonding characteristics such as the intensity and the longevity of intra- and intermolecular hydrogen-bonded pairs are examined for the first time in these systems. It was found that the volume fraction of the penetrating solvent molecules increased upon decrease of pH, but no dependence on the size of the molecules was observed. The density of the solvent within the dendritic interior did not exceed that of the bulk, while the corresponding number of counterions entering the dendrimer boundaries exhibited a marked increase between the 3rd and the 4th generation of the dendrimers. Intramolecular hydrogen bonding was favored at high pH conditions, while intermolecular hydrogen bonding between PAMAM and the solvent or the PEO was significantly enhanced upon protonation of the dendrimer's amines. The presence of PEO imparted appreciable changes in the dendrimer's shape particularly in the physiological pH conditions. In addition, it incurred a decrease in intramolecular hydrogen bonding and acted antagonistically to the formation of water/dendrimer hydrogen bonds. The higher degree of hydrogen bonding between PAMAM and PEO was observed at low pH levels, indicating that under these conditions the formed complexes are expected to be more stable. The findings of the present study were found to be in good agreement with the relevant experimental findings where available, thus assessing the role of several structural and conformational details in the manifested behavior and providing further insight of the effects of non-covalent complexation of PAMAM dendrimers with linear poly(ethylene oxide).

I. Introduction

Dendrimers are synthetic polymers that consist of a central core, to which radially attached branching units lead to a spherical periphery of a well-defined number of terminal groups. Due to their structural characteristics (nanosize dimensions, controlled size and shape, multifunctionality) they are suitable candidates for numerous biomedical applications.[1,2] A family of dendritic polymers frequently utilized in such applications are polyamidoamine (PAMAM) dendrimers. Due to their ionizable amine groups, different charging states can be attained, thus providing the means for controlling aspects of their physicochemical behavior. Studies in PAMAM aqueous solutions suggest that the dendritic structure undergoes characteristic changes under varying pH conditions and ionic strength of the solution.[3–7]

Apart from changes in the overall size, modifications in the intra-dendrimer density distribution which involve relocation of terminal groups[8,9] and increase or decrease of the percentage of internal cavities,[10] may significantly affect the ability of these molecules to , *e.g.*, act as hosts to molecules of pharmaceutical interest[11,12] or to form complexes with other polymers of synthetic[13] or biological[14] nature. Recent experiments indicated that electrostatic repulsion between primary or tertiary amines driven by changes in the solution's pH, can promote the encapsulation of small compounds into PAMAM internal voids.[15,16] It has also been demonstrated that the availability of free space within the dendritic structure combined with hydrogen bonding interactions between PAMAM amine groups and hydrophobic moieties, are among the key factors for entrapment of poorly soluble molecules into the dendrimer interior.[17–19]

Physical Chemistry Laboratory, Chemical Engineering Department, Aristotle University of Thessaloniki, 54124 Thessaloniki, Greece. E-mail: karatas@eng.auth.gr; Fax: +30-2310996222; Tel: +30-2310995850

† Electronic supplementary information (ESI) available: Spectra for dendrimers and linear chains reflecting the correlation functions of the squared radius of gyrations for the dendrimer (G3 and G4 models) and linear PEO (G3 and G4 models) molecules. See DOI: 10.1039/b913986a

A category of systems based on PAMAM dendrimers which are utilized for biomedical as well as numerous industrial purposes, involve the formation of complexes with polymeric molecules which are covalently bonded or non-covalently associated (*i.e.*, *via* hydrogen-bonding or electrostatic interactions)[20–23] with dendrimers. Recent findings suggest that cytotoxicity of cationic PAMAM dendrimers subsides upon addition of polyethylene oxide (PEO) chains.[24] For example, surface positive charges of cationic dendrimers are shielded by the presence of linear chains, resulting in the reduction of undesired interactions with charged cell membranes, thus facilitating the transfer of genetic material into the cell.[25] In addition, the presence of PEO chains in the vicinity of the dendritic structure results in increase of the load of otherwise poorly soluble drugs into dendrimer cavities.[26,27] The stability and response of the formed complexes in different solution conditions, were found to be linked to attributes such as the size of the dendrimer, the nature of the solvent and the degree of its penetration within the dendrimer, as well as the extent of hydrogen-bonding formation involving dendrimer functional groups.[4,23,28–32]

The aim of the present study is to provide a more detailed account of the role of certain aforementioned factors in the behavior of specific dendrimer systems which are among those most frequently used for complexation purposes with other polyelectrolytes of synthetic or biological nature. Namely, we have studied static and hydrogen-bonding aspects of dendrimer's behavior in aqueous solutions by means of fully atomistic molecular dynamic simulations, exploring the effects of the presence of linear PEO chains, of the dendrimer size and of the pH of the solution. More specifically, static properties pertinent to the dendrimer conformational and geometric details as well as to the degree of solvent and counterion penetration are examined, while characteristic intra- and intermolecular hydrogen bonded pairs are also explored both from a static and dynamic point of view.

Since we only considered complexed models comprised of a single PEO chain, the part of this study referring to PAMAM/PEO systems should be viewed as a first step toward a more detailed assessment on possible changes in dendrimer's static/conformational as well as hydrogen-bonding characteristics, due to the presence of a non-ionic hydrogen-bonding-capable linear chain in its close vicinity. Although a more realistic description would involve the presence of several linear chains near the dendrimer, the following approach may provide a useful starting point by isolating the single-chain effects, as has been described in other analogous cases (for instance, in PAMAM/DNA complexation[23]). Moreover, the fully atomistic nature of the simulations is a step forward as compared to past efforts describing dendrimer/linear polymer complexes in coarse-grained representations,[33–35] where specific interactions such as hydrogen bonding were not considered.

II. Simulation details

According to titration experiments,[36] at high pH, PAMAM dendrimers possess zero total charge, whereas at physiological pH all primary amines are protonated. Further decrease of solution's pH (*i.e.* pH $\sim$ 4) is accompanied by protonation of the tertiary amines too. To mimic high, neutral and low pH conditions as described above, the dendrimers' amines were either left unprotonated (high pH), only the primary amines were protonated (neutral pH), or primary and tertiary amines were both protonated (low pH).

We have examined ethyldiamine (EDA)-cored systems of the 3rd (G3) and the 4th (G4) generations, with, or without the presence of a linear PEO polymer. Each system was comprised by one dendrimer molecule and one PEO chain (in systems where the linear polymer was present) in explicit water solutions, mimicking dilute solution conditions where the number density of both polymer species are comparable. In dendrimer/linear polymer systems, the number of monomers of the PEO chain was chosen to be equal to the number of the terminal amine groups of the corresponding dendrimer.

Among all possible choices for the chain length of PEO, we opted for this selection for two reasons: on one hand by taking into account the scaling of the size of the PEO chains[37] and that of the PAMAM dendrimers[6] in an aqueous environment, we expected that by this choice the dimensions of the two molecules would be comparable. In this manner the linear chain could explore a significant percentage of the dendrimer's surface, as was demonstrated in a previous work on PAMAM/DNA complexes;[23] on the other hand, by following this approach, the number of the hydrogen-bonding-capable sites of PEO (*i.e.*, oxygens) would match the number of the surface amine groups of the dendrimer , thus, preserving a stoichiometry between the functional sites of the two molecules in a sense similar to the procedure followed in relevant experiments (*i.e.*, in dendrimer/DNA complexation where the phosphate groups of the nucleid acid were chosen to be at an equinumber concentration with the dendrimer surface amine groups[14,20]). The details of the 12 systems studied are listed in Table 1.

The initial configurations of G3 and G4 neutral PAMAM dendrimers were obtained from an earlier simulation study.[38] In the cases of PAMAM/PEO systems, the PEO chain was placed close to the dendrimer periphery (the average center of mass distance between dendrimer and PEO chains was $\sim$20 Å, in order to mimic the state of a dendrimer/PEO complex).

At the first stage in the construction of the models, the polymers (dendrimer plus PEO if present) were subjected to steepest descent and conjugate-gradient energy minimization cycles (typically of the order of 40 000 steps) in vacuum, utilizing energetic parameters according to the AMBER[39,40] forcefield including terms describing bond-stretching, angle-bending, torsional rotation, van der Waals, hydrogen-bonding and electrostatic interactions (eqn (1))

$$E_{\text{total}} = \sum_{\text{bonds}} K_R(R - R_0)^2 + \sum_{\text{angles}} K_\theta(\theta - \theta_0)^2 + \sum_{dih.} \frac{V_n}{2}[1 + \cos(n\phi - \delta)] + \sum_{i<j} \left[\frac{A_{ij}}{R_{ij}^{12}} - \frac{B_{ij}}{R_{ij}^{6}}\right] + \sum_{\text{H-bonds}} \left[\frac{C_{ij}}{R_{ij}^{12}} - \frac{D_{ij}}{R_{ij}^{10}}\right] + E_{\text{elec.}} \quad (1)$$

In the second stage, PAMAM dendrimers/complexes were hydrated in cubic cells the dimensions of which were chosen

Table 1 Details of the simulated systems. The notations "basic", "neutral" and "acid" refer to the pH condition characterizing each system. The "PEO" term refers to systems where a linear PEO chain is present

Systems' notation	Total number of atoms per dendrimer	Dendrimer charge
G3_basic	1092	0
G3_neutral	1124	32
G3_acid	1154	62
G3_PEO_basic	1092	0
G3_PEO_neutral	1124	32
G3_PEO_acid	1154	62
G4_basic	2244	0
G4_neutral	2308	64
G4_acid	2370	126
G4_PEO_basic	2244	0
G4_PEO_neutral	2308	64
G4_PEO_acid	2370	126

to provide at least a 10 Å solvation shell around the dendrimer/complex structure.[6,41] Energetic parameters for water molecules were assigned according to the TIP3P model.[42] To preserve the overall charge neutrality and to represent more realistic conditions, an appropriate number of Cl^- counterions was added in neutral and low pH systems (inclusion of explicit counterions influences significantly the structure and dynamics of charged dendrimers as reported in earlier studies[43–46]). Partial charges to the dendrimer/PEO molecules were assigned following the Gasteiger[47] method while all electrostatic interactions were evaluated by full Ewald summation. A cut-off radius of 10 Å was applied for the van der Waals interactions which were described by a 12–6 Lennard-Jones potential, while hydrogen bonding interactions between hydrogen-acceptor pairs were evaluated by a 12–10 potential term.[39]

The 3rd stage of the simulation protocol, involved equilibration runs of 200 ps using a 0.1 fs timestep, followed by several hundred ps (with a timestep of 1 fs) at the isobaric-isothermal ensemble (p = 1 bar, T = 298 K) in order to allow the system to come to an equilibrium after introduction of water and counterions (all MD runs were performed in a cubic box with periodic boundary conditions). At the end of this procedure, the total energy, the dendrimer and linear chain radii of gyration, the specific volume of the systems and the distributions of water molecules and counterions around the dendrimers, were stabilized.

Finally, starting from the configurations produced by the above procedure, production runs of 4–6 ns trajectories with a 1 fs timestep were performed in the constant-volume constant-energy ensemble (NVE) at room temperature. At times below 1 ps, data were collected at every other timestep, whereas at longer times the saving frequency was increased to 1ps.

The forcefield adopted (AMBER), has been successfully applied in past computational studies[19,48,49] for the description of PAMAM dendrimers, while its combination with TIP3P parameters for water molecules was found to adequately describe not only fully atomistic PAMAM/water systems[19,49] but also aqueous solutions of more complex biological molecules.[23,50,51] In addition, as has been demonstrated in recent simulational efforts involving systems of biological interest[52–54] or hyperbranched molecules,[55] assignment of partial charges according to the Gasteiger method in conjunction with the utilization of the AMBER forcefield, resulted to a fair description of their physicochemical behavior. Therefore, for consistency purposes, we have also used the AMBER forcefield and the Gasteiger method to model PEO chains as well. To verify the appropriateness of this approach in the description of PEO behavior in an aqueous environment, we have constructed and simulated (using a similar protocol as above) models comprised by single PEO chains in TIP3P water (polymer weight fraction $w_p \approx 0.03$), of molecular weight identical to the ones invoked in the dendrimer systems. Calculation of the average radii of gyration of PEO chains in these systems rendered R_g values of 11.2 ± 0.9 Å and 14.7 ± 0.8 Å for the 32 and the 64 monomer chains respectively, which are in a close accord with recent literature data for aqueous PEO solutions[37,56] (after extrapolation to the examined molecular weights). Furthermore, the hydration layer around PEO chains as was determined from the pair correlation function between PEO ether oxygens and water hydrogens (~2.7 Å), was also found to be in agreement with that estimated from previous computational studies.[57]

To check that the length of the produced trajectories was sufficient for the conformational relaxation of the polymeric components of the systems, we evaluated the time correlation function of the fluctuations of the squared radius of gyration (R_g)[58] and verified that in all examined systems of Table 1, it had decayed to 0 at timescales no longer than 1 ns (see ESI).†

Fig. 1 depicts snapshots of all the models studied (water molecules and hydrogen atoms are omitted for clarity). In all cases each simulation box was several times (between 3 to 5 times) larger compared to the radius of gyration of the dendrimer molecule (the largest radii of gyration amounted to 18.5 ± 0.3 Å and 22.6 ± 0.7 Å for the fully protonated G3 and G4 models, respectively).

The average dimensions of the linear chains (if present), were smaller compared to the companion dendrimer and remained practically unchanged at the high and physiological pH conditions (approximately 10.8 ± 1.0 Å in G3 and 13.1 ± 1,0 Å in the G4 systems), whereas they exhibited an increase of about 5% for the G3 and 30% for the G4 systems at the low pH regime.

III. Results on statics

A Effects on the dendrimer shape parameters

An informative way to describe shape characteristics of polymers and in particular for the characterization of the

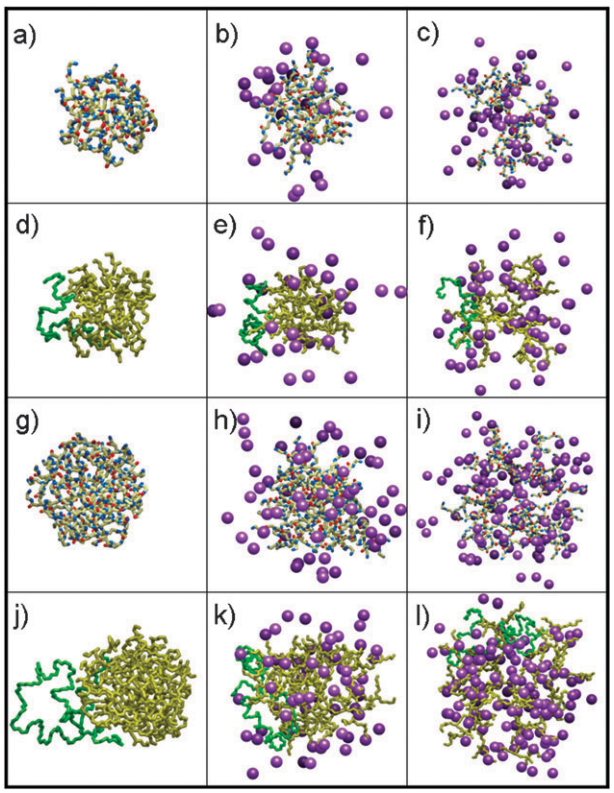

Fig. 1 Snapshots of the simulated systems (a) G3_basic (b) G3_neutral (c) G3_acid (d) G3_PEO_basic (e) G3_PEO_neutral (f) G3_PEO_acid (g) G4_basic (h) G4_neutral (i) G4_acid (j) G4_PEO_basic (k) G4_PEO_neutral (l) G4_PEO_acid. In systems with PEO present, the dendrimer and the linear chain are shown in different colors. Counterions are shown in purple. In systems without PEO, carbons are shown in yellow, nitrogens in blue and oxygens in red. Hydrogens and water molecules are omitted for clarity. Systems' notation follows that of Table 1.

geometrical features of dendrimer molecules, is the determination of the principal moments ($I_z > I_y > I_x$) of the shape tensor G

$$G_{mn} = \frac{1}{M}\sum_{i}^{N} m_i(r_{mi} - R_m)(r_{ni} - R_n)\ m,n = x,y,z \qquad (2)$$

and the relative aspect ratios (I_z/I_x, I_z/I_y) of the equivalent ellipsoid.[6,38,59] In eqn (2), R is the position of the center of mass and M the total mass of the dendrimer.

To quantify the degree of deviation of dendrimer's shape from that of a sphere using a single parameter, we additionally evaluated the asphericity parameter δ (also termed as relative shape anisotropy), which is defined as[61]

$$\delta = 1 - 3\frac{\langle I_2\rangle}{\langle I_1^2\rangle} \qquad (3)$$

where $I_1 = I_x + I_y + I_z$ and $I_2 = I_xI_y + I_xI_z + I_yI_z$. Parameter δ ranges between 0 and 1 which corresponds to a spherical (*i.e.*, a shape of high symmetry) and a rod-like geometry respectively. The aspect ratios of the PAMAM molecules and the corresponding asphericities of all the studied models are listed in Table 2.

Table 2 Aspect ratios and asphericities of the dendrimer molecules

System	I_z/I_x	I_z/I_y	δ
G3_basic	1.62 ± 0.15	1.26 ± 0.13	0.020 ± 0.007
G3_neutral	1.88 ± 0.20	1.24 ± 0.11	0.031 ± 0.009
G3_acid	1.63 ± 0.22	1.24 ± 0.14	0.033 ± 0.016
G4_basic	1.44 ± 0.16	1.14 ± 0.07	0.011 ± 0.006
G4_neutral	1.66 ± 0.23	1.26 ± 0.16	0.022 ± 0.011
G4_acid	1.46 ± 0.16	1.16 ± 0.09	0.012 ± 0.006
G3_PEO_basic	1.74 ± 0.30	1.22 ± 0.10	0.025 ± 0.013
G3_PEO_neutral	2.55 ± 0.38	1.33 ± 0.14	0.061 ± 0.016
G3_PEO_acid	1.59 ± 0.22	1.26 ± 0.17	0.014 ± 0.007
G4_PEO_basic	1.61 ± 0.14	1.25 ± 0.11	0.019 ± 0.007
G4_PEO_neutral	2.36 ± 0.20	1.39 ± 0.09	0.053 ± 0.009
G4_PEO_acid	1.80 ± 0.32	1.26 ± 0.11	0.023 ± 0.011

The aspect ratios characterizing the shape of dendrimers, do not exhibit any systematic trend on the degree of protonation, and their values (at least as far as it concerns the G4 models for which data at different pH levels are available) are in reasonable agreement to past relevant studies.[6] The larger size (G4) models exhibit on average somewhat lower ratios, in agreement with earlier findings in dendrimer systems.[6,38,60]

The presence of the linear chain results to the increase of the degree of anisotropy in the shape of dendrimers as it is also implied by the increase of the pertinent aspect ratios. The larger generation (G4) models, exhibit on average a somewhat lower deviation from the spherical geometry compared to the G3 systems. The changes induced due to the presence of linear PEO appear to be more significant in the neutral pH case.

B. Effects on intra-dendrimer atomic arrangements

Knowledge of the intra-dendrimer atomic arrangements combined with information regarding solvent or counterion penetration within the dendritic structure, is of particular importance in applications *e.g.* associated with the entrapment of other molecular moieties within the dendrimer interior. To characterize our systems in this respect we have constructed the radial density distribution functions associated with the dendrimer atoms, the water molecules and the counterions, with reference to the center of mass of the dendrimer molecule.

Fig. 2 depicts the aforementioned density profiles for all the examined systems. The dendrimer profiles refer to the overall average density.

As can be inferred upon inspection of Fig. 2a and d (non-protonated systems), for both size dendrimers, apart from the somewhat higher density at a distance close to the centers of mass corresponding roughly to a bond length (to a good approximation the center of mass is very close to the location of the dendrimer core), the average dendrimer profiles exhibit a plateau-like behavior followed by a monotonic drop near the dendrimer's periphery. These features are consistent with observations made in relevant experiments[62,63] and computational studies in PAMAM systems.[6,38,64] The plateau value of the density appears to be independent of the dendrimer size. For systems of both sizes, the solvent penetration is limited to the area of the dendrimer's periphery as implied by the location where overlap between the respective distributions occurs. Introduction of the linear PEO chain does not practically affect the main features of the profiles as described above.

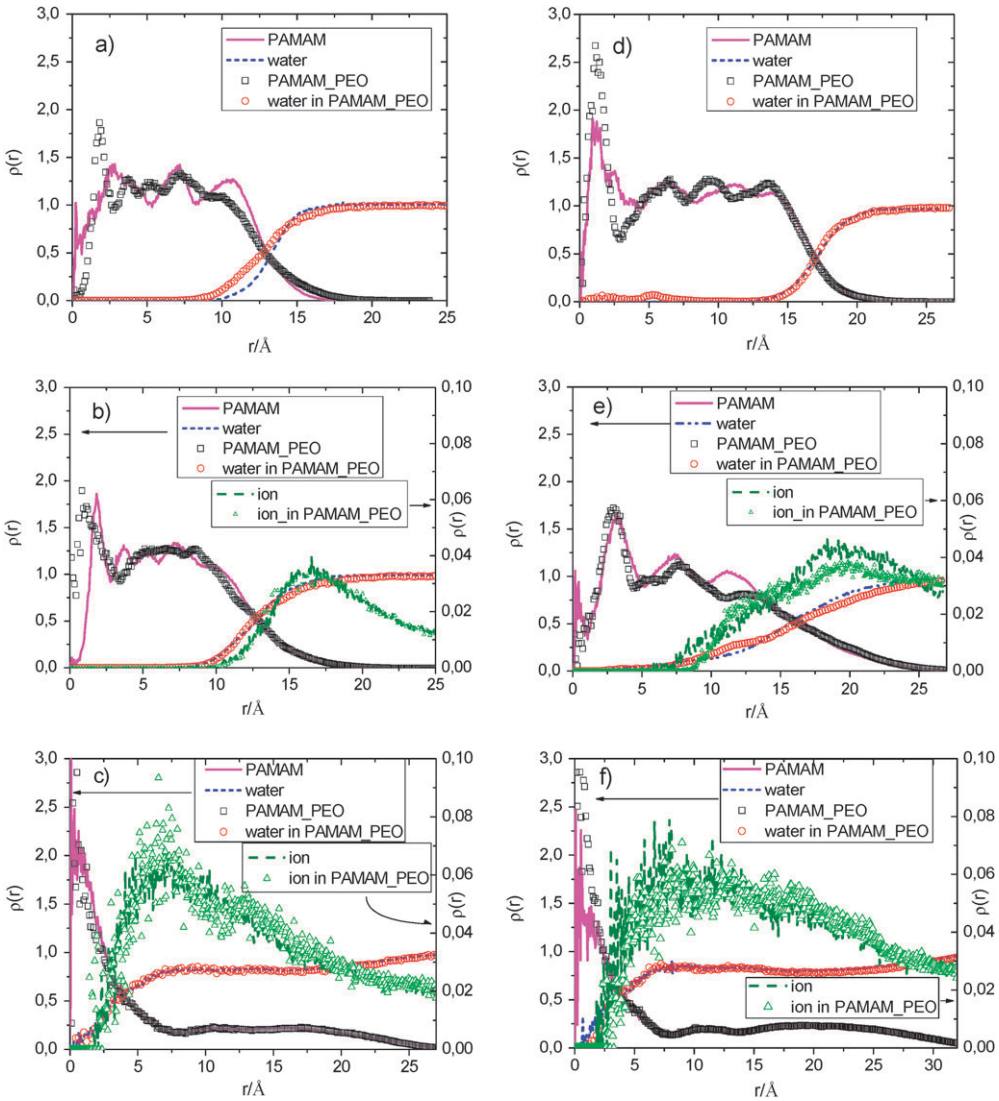

Fig. 2 Radial density profiles of generation G3 (a), (b), (c) and G4 (d), (e), (f) systems of PAMAM, water and counterions. pH level decreases from top to bottom.

At neutral pH conditions (Fig. 2b and 2e) where the primary amines are protonated, certain differences appear between models of the two generations. At the smaller generation dendrimer (G3) the plateau value of the density is only marginally affected compared to the non-charged state (Fig. 2a). On the other hand, at the largest size dendrimer (Fig. 2e) the effects of protonation of the primary amines are more pronounced. Not only the plateau level is lower compared to the respective non-charged model (Fig. 2d), but also the profile is appreciably broadened toward the dendrimer's periphery resulting to a more gradual drop of the density. As can be inferred by inspecting the corresponding counterion density profiles, at G4 systems the latter assume a significantly broader shape indicating a larger degree of penetration within the dendritic structures compared to the analogous profiles describing the G3 systems.

This picture is consistent with a more "open" structure in the G4 dendrimers which would allow an increased accessibility of the dendrimer's interior. It is also compatible with the considerably broader profiles associated with the water density distributions observed in these systems. The same feature may also rationalize the fact that the presence of the PEO chain appears to affect to a certain degree the density profiles of the G4 systems, whereas in the G3 systems such an effect is practically negligible. At low pH conditions, the changes in the dendrimer density profiles are dramatic for models of both generations. A rather compact core region is formed, followed by an extended plateau-like profile at a density level of almost half as compared to higher pH states, in line with the behavior observed in larger dendrimer models.[6] Other characteristic features at the low pH state which are consistent with a larger degree of "openness" of the internal structure, are the homogenous distribution of water molecules throughout the dendrimer interior at distances further from the formed core, as well as the maximization of the counterion density distributions somewhat further from the core region.

In all cases the average water density did not exceed that of bulk water. In particular, at the fully protonated state the

corresponding profiles appear almost flat at distances away from the center and the periphery of the dendrimer. This information provides new insight concerning an issue raised from experimental studies in aqueous PAMAM solutions, as to whether the water density in dendrimer's interior remains below or exceeds the bulk value.[10] The above observation does not actually contradict the rather elevated volume fraction of water molecules which has been observed at relevant small angle neutron scattering (SANS) experiments in aqueous PAMAM solutions.[10] In the latter experimental work,[10] it has been demonstrated that the volume fraction occupied by penetrating water molecules with respect to the dendrimer volume, can be as much as 50% or higher. According to these experiments (only neutral dendrimer systems were studied), the volume fraction of the penetrating solvent exhibited a rather weak dependence on the size of the dendrimer (systems of generations 4 to 6 were examined).

To compare the above observations to our results for the non-charged models and to examine in which manner the changes in pH (*i.e.* protonation of the PAMAM dendrimers) and the presence of the linear chain affect this behavior, we have calculated the relative volume fraction occupied by the solvent and the counterions, as listed in Table 3. In this calculation (based also on the almost spherical shape of the dendrimers as discussed earlier), we have taken as the radial boundary of a dendrimer (denoted henceforth as R_{dend}) the distance at which the dendrimer density profiles drop to zero. At the same distance the density profiles of water attain the bulk value as well (see Fig. 3). The corresponding volume fractions have been estimated by evaluating the ratios $\varphi_{wat} = V_{wat}/V_{dend}$ and $\varphi_{Cl^-} = V_{Cl^-}/V_{dend}$ where $V_{Cl^-} = \frac{4}{3}\pi r_w^3 N_{Cl^-}$ and $V_{wat} = N_{wat} \times v_{wat}$. In the latter expressions, N_{wat} and N_{Cl^-} are the number of penetrating water and counterions, respectively, while v_{wat} represents the volume of a single water molecule (taken as 30 Å^3)[10] and r_w the van der Waals radius of the chlorine ion (here $r_w = \sigma_{LJ}/2 = 2.47$ Å).

As a general trend, it appears that protonation of PAMAM dendrimers increases the relative volume occupied by the water molecules, in line with the picture described earlier regarding the larger availability of accessible space in the dendrimer's interior.

For the non-protonated models, the volume fraction of water for the G4 system is in very good agreement with the experimentally determined value[10] (*i.e.* 0.45 ± 0.05) when scattering data are fitted with a hard-sphere model with radius moderately larger than R_g.

Table 3 Volume fraction of counterions and water molecules with respect to the volume included within the dendrimer boundary (see text)

	φ_{wat}			φ_{Cl^-}	
System/pH	High	Neutral	Low	Neutral	Low
G3	0.54	0.72	0.90	0.024	0.029
G4	0.50	0.77	0.86	0.034	0.035
G3-PEO	0.54	0.69	0.89	0.023	0.030
G4-PEO	0.55	0.73	0.79	0.031	0.037

The experimentally observed weak dependence of the solvent-occupied volume fraction on the dendrimer generation,[10] is noted in the simulation results for the protonated dendrimer models as well. On the other hand, a notable increase is observed on the volume occupied by the counterions when moving from the G3 to the G4 models. This notion is consistent with recent SANS experiments in G3-G6 PAMAM dendrimers[65] at varying protonation levels, where it has been reported that the effective charge rises with generation and exhibits the largest increase from G3 to G4 dendrimers.

The presence of the PEO chain does not practically affect the behavior noticed in the dendrimer–water systems.

C Pair distribution functions of hydrogen-bonded pairs

Non-covalent interactions driven by atoms that can act as proton donors or acceptors in hydrogen-bonded pairs have a marked impact on the conformations adopted by PAMAM dendrimers as well as in their solution behavior.[49] Many applications of PAMAM dendrimers ranging from fabrication of thin films[66] to binding of semiconductor nanocrystals[67] are dominated by hydrogen bond formation. Moreover, the potential of PAMAM dendrimers to act as hosts for hydrophobic drug compounds has frequently been attributed to the formation of hydrogen bonds between PAMAM and appropriate drug groups.[18,68] To elucidate aspects of hydrogen bonding interactions of PAMAM dendrimers either at intra- or intermolecular level, we have evaluated pair distribution functions between hydrogens attached to atoms which act as proton donors and atoms acting as proton acceptors.

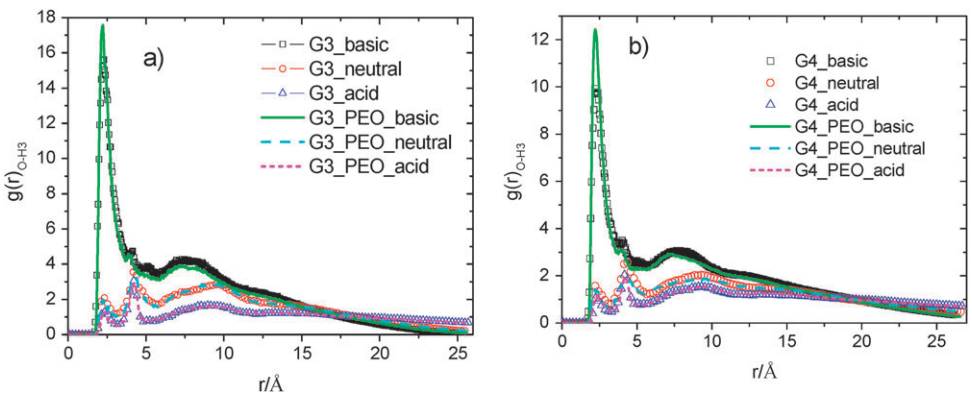

Fig. 3 Intramolecular pair distribution functions of primary amine hydrogen–carbonyl oxygen for G3 (a) and G4 (b) systems.

Namely, between PAMAM carbonyl oxygen (O), primary amine hydrogen (H3), PEO ether oxygen (OE), water hydrogen (HW) and water oxygen (OW). The criteria we adopted for the definition of a hydrogen bond were based on the hydrogen–acceptor distance as well as on the angle formed by the donor–hydrogen–acceptor triplet. The maximum distance considered, was the one corresponding to the first minimum of the relevant hydrogen–acceptor pair distribution function, while the minimum donor–hydrogen–acceptor angle was selected to be 120°.[49,69,70]

C.1 Intramolecular hydrogen bonding. Intramolecular hydrogen bonds have been experimentally observed by NMR techniques in PAMAM dendrimers through analysis of the nitrogen chemical shifts of amines. Simulations results in poly(propyleneimine) dendrimers, attribute a significant amount of backfolding of terminal groups to the hydrogen bonds formed between primary (*i.e.*, peripheral) amines and sites located in the interior of the dendritic structure.[71] Prompted by the significance regarding the extent of intramolecular hydrogen bonding in dendrimers, we have explored hydrogen bonding formation between a characteristic pair, namely the primary amine hydrogen (H3) and the carbonyl oxygen (O), on accounts of the geometric criteria mentioned earlier. Fig. 3 presents corresponding correlation functions of the H3–O pair in all the examined models. A sharp peak at a separation $\sim$2.2 Å is observed in non-protonated systems, which can be assigned to hydrogen bonding.[70]

Protonation of primary amines either at physiological or at acid pH conditions decreases significantly the probability of intramolecular hydrogen bond formation (note the large drop in the amplitude of the respective peak).

This observation is consistent with the fact the protonation of amines is responsible for their stretching-out toward the dendrimer periphery and therefore for the decrease (but not total inhibition) of their backfolding.[6] Lowering the degree of backfolding would also lower the probability for a close proximity of intramolecular H3–O pairs, and thus the formation of hydrogen bonds between them.

Fig. 4 shows the average number of the H3–O hydrogen-bonded pairs per H3 site per timeframe (here 1 ps). Indeed, a drop of the order of 80% or higher is observed at neutral or low pH conditions with respect to the high pH state. In the fully protonated state, the average number of intramolecular H3–O hydrogen bonds appears to have dropped to almost half the amount characterizing the neutral pH state. The effect of dendrimer generation appears to be only minor; in the charged models (*i.e.* at neutral and low pH), the degree of hydrogen bonding between the examined pairs is slightly higher in the G4 systems. The presence of linear PEO appears to incur only a small increase in the intramolecular hydrogen-bond formation involving O–H3 pairs, which is more apparent in the basic and acid pH G4 systems.

C.2 Intermolecular hydrogen bonding. As noted earlier, hydration of the dendrimer is characterized by a marked degree of penetration of water molecules into the molecule's interior. Simulation studies have shown that water molecules confined in supramolecular assemblies or close to a polyelectrolyte exhibit slower solvation dynamics compared to bulk water.[41] Apart from steric hindrance reasons, to a large degree water molecules remain associated within the macromolecular structure due to hydrogen bonding and electrostatic interactions.[72,73] Since hydration interactions can play a significant role in the physicochemical processes associated with the behavior of biological molecules,[74] and in particular as far as their complexation with dendrimers are concerned,[23] it is of interest to examine aspects of hydrogen bonding between dendrimers and water molecules. To compare with the behavior of a hydrogen atom participating also in intramolecular hydrogen bonding, we have evaluated the radial distribution functions between primary amine hydrogen (H3) and water oxygen (OW) for the examined models, as shown in Fig. 5.

At high pH conditions a low-amplitude peak at $\sim$2.5 Å can be observed for both generation systems. At protonated systems however, the appearance of a sharp peak at a distance of $\sim$1.9 Å indicates that hydrogen bonding between the primary amine hydrogens and water is stronger compared to high pH conditions.[70]

Quantification of this difference is made by calculation of the average number of hydrogen bonds per H3 atom, as presented in Fig. 6. Comparison between the protonated systems shows that the degree of hydrogen bonding corresponding to the H3–OW pair, is independent both of dendrimer size and solution pH, while the hydrogens of the primary protonated amines participate on average in more than one hydrogen bonds with water molecules. The presence of the linear chain, results approximately to a 3 and 5% decrease of the number of the examined hydrogen bonds in the protonated G3 and the G4 models respectively.

In the non-protonated systems H3–OW hydrogen-bonding does not seem to change in a systematic manner after the introduction of the PEO chain (in G4 systems it remains practically unaffected whereas in the G3 systems it is increased). The small decrease observed in protonated systems (*i.e.*, 3 to 5%), can be ascribed to an antagonistic (against water) action of the PEO chain in forming hydrogen bonds with the primary amine hydrogens.

To check the extent of hydrogen bonding between dendrimer and linear chain, we have also examined the pair distribution functions between the dendrimer's primary amine hydrogen, H3, and PEO ether oxygen (OE), as shown in Fig. 7. Evidently, the examined hydrogen bond pairs between PAMAM and PEO are formed solely at low and neutral pH conditions. This behavior is consistent with the fact that when the amines are protonated (*i.e.* when charged groups are present), hydrogen bond formation is more probable.[70] The presence of hydrogen bonds between PEO and PAMAM dendrimers at physiological and low pH conditions, is therefore an indication for the formation of more stable complexes. Among the protonated systems, there appears to be a pH effect which amounts to an almost 50% increase of the examined pairs at low pH systems. As mentioned earlier (see Fig. 3), at low pH conditions the degree of intramolecular hydrogen bonding in dendrimers is minimized allowing also an easier access of the linear polymer to the outer amine groups.

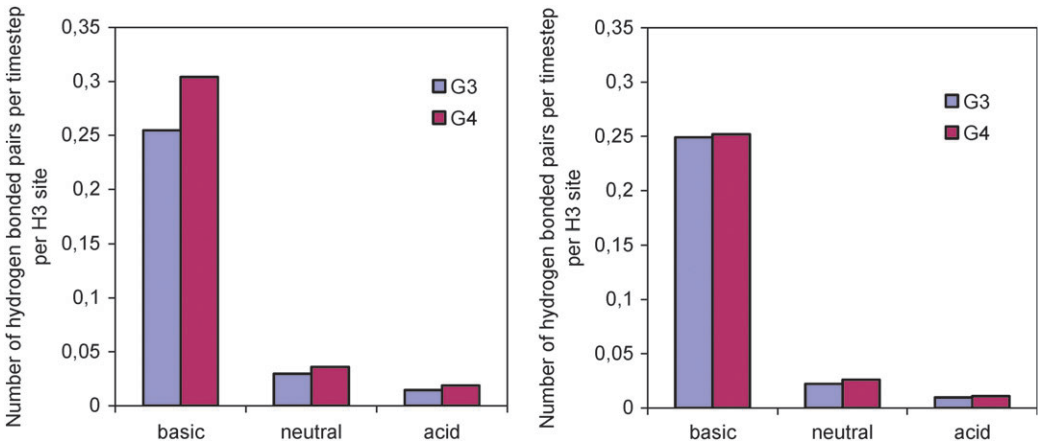

Fig. 4 Average number of hydrogen bonded intramolecular O-H3 pairs per time frame per H3 site, with (left), or without (right), the presence of the linear PEO chain, at different pH conditions.

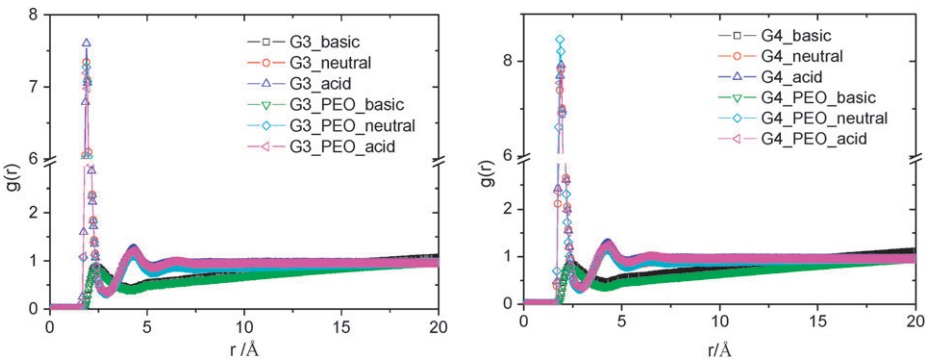

Fig. 5 Intermolecular pair distribution functions between primary amine hydrogen and water oxygen for G3 (left) and G4 (right) systems.

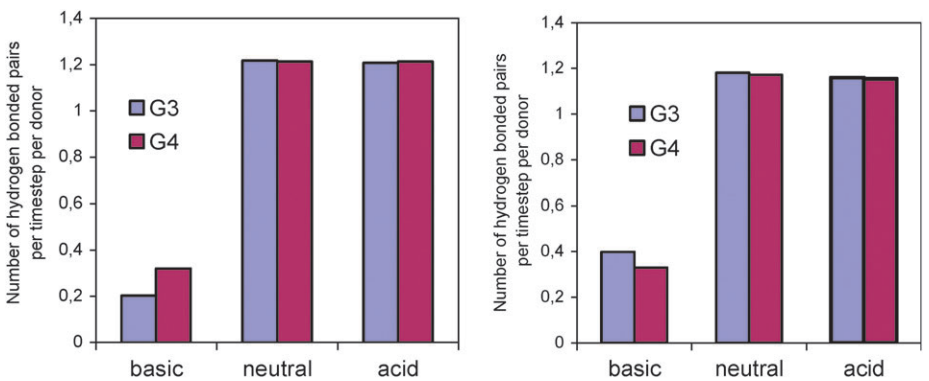

Fig. 6 Average number of hydrogen bonded intermolecular H3–OW pairs per time step per H3 site for systems with (right) or without (left) the presence of PEO, as a function of pH.

Fig. 8 depicts the average number of H3–OE hydrogen bonded pairs, in the low and neutral pH conditions. There is no apparent differentiation between models of the two dendrimer sizes.

In addition, the protonation of the primary amines increases the probability for hydrogen-bond formation between the amine hydrogens and the PEO acceptor sites.

These effects, combined with the noted decrease of the (counteractively acting) H3–OW hydrogen bonding observed in the low pH models (Fig. 6), may rationalize the larger degree of hydrogen bond formation between the dendrimer primary amines and the linear chain in this pH regime.

IV. Hydrogen bond dynamics

To explore the dynamics of hydrogen-bonding pairs at a wider temporal window, we also produced trajectories and collected data every 2 fs at the subpicosecond range. Hydrogen-bonded pair dynamics were explored by evaluating a survival probability function defined as[75]

$$P(t) = \frac{\sum_{(i,j)} p_{ij}(t)}{\sum_{(i,j)} p_{ij}(t=0)}$$

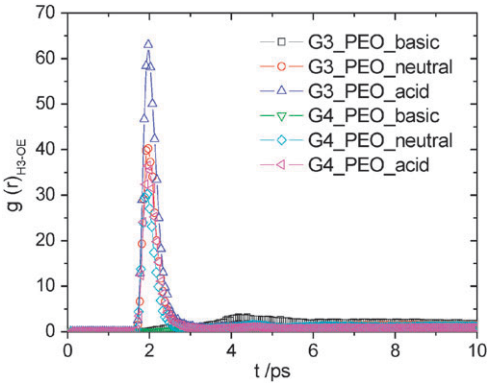

Fig. 7 Pair distribution function between PAMAM primary amine hydrogen (H3) and PEO ether oxygen (OE)

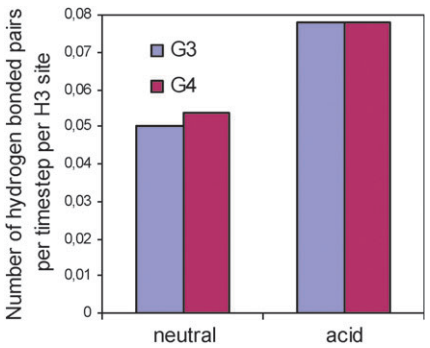

Fig. 8 Average number of hydrogen bonded PAMAM primary amine hydrogen (H3) and PEO ether oxygen (OE) pairs per timestep per H3 site at neutral and acidic pH levels.

where $p_{ij}(t)$ takes the value of 1 if the hydrogen bond that exists between the ith and the jth atoms at $t = 0$ survives at time $t > 0$ and 0 otherwise. The summation runs over all atomic pairs found to form a hydrogen bond at $t = 0$ (all different time origins have been taken into account). Average hydrogen bonding lifetimes were evaluated by integration of the corresponding survival probability functions. It must be noticed here that the so-calculated average residence times reflect mainly the long-time behavior of the relevant probability functions (*i.e.* the subpicosecond breaking/recombination of hydrogen bonds[55,72,76] is not expected to be clearly resolved as a separate process following this analysis). Notwithstanding, in most of the potential applications in which such systems are intended to be used, information regarding the long-time behavior is of key importance.

To obtain an idea regarding the different timescales associated with intra- or intermolecular hydrogen bonded pairs, we have examined the O–H3 (intramolecular) and H3–OW (intermolecular) pairs, for which we have presented earlier relevant static data.

Fig. 9 illustrates the hydrogen bonding survival correlation functions arising from intramolecular O–H3 pairs for all the examined systems. For both size models, $P(t)$ indicates that the slower dynamics correspond to high pH conditions (note the decay of the probability function at longer times), while protonated systems exhibit a similar dynamic behavior. The presence of PEO does not seem to induce a noticeable effect. The probability functions describing the behavior of the intermolecular H3–OW pair are shown in Fig. 10.

Evidently, for both generation systems, hydrogen bonds that are formed at high pH conditions are shorter lived (*i.e.* $P(t)$ decays at earlier times) compared to those formed at neutral and low pH systems. The characteristic lifetimes corresponding to the intra- and intermolecular hydrogen-bonding residence functions shown in Fig. 9 and 10, respectively, are plotted in Fig. 11.

As a general observation one can note that independently of the dendrimer generation, the time describing the residence period of the intramolecular pairs decreases upon protonation of the primary amines. Subsequent protonation of the tertiary amines (*i.e.*, at low pH conditions), only slightly affects (decreases) the lifetime of the H3–O pairs. On the other hand, the lifetime of the intermolecular H3–OW pairs increases upon protonation, whereas at the low pH conditions only a minor decrease in residence time is observed with respect to the neutral pH state. This behavior corroborates the scenario regarding the competition between intra- and intermolecular hydrogen bonding which has also been implied by the variation of the average number of pertinent bonded pairs (Fig. 4 and 6).

The presence of linear PEO results to certain deviations from the times characterizing the systems without the linear chain, but the general behavior remains unchanged.

Comparing the timescales describing the intra- and the intermolecular pairs, it is apparent that residence times of the H3–O intramolecular pairs are always longer than those between the primary amine hydrogens and water. This could be attributed partly to the fact that the carbonyl oxygens are located not only at the topological extremities of the dendrimer structure but also at sites within the molecule's interior. Since the timescale for local conformational changes increases from the periphery to the core,[60,77–79] it is reasonable to assume that once hydrogen-bonded pairs are formed at inner sites, they sustain a higher probability to remain intact for longer times. As has been recently demonstrated,[55] dynamics of intramolecular hydrogen-bonded pairs in hyperbranched molecules can be coupled to relatively slow internal molecular motions. Such a coupling would tend to increase the lifetimes of intramolecular hydrogen bonded pairs. For instance, in the case of non-protonated systems, a timescale of the order of 100 ps which characterizes the residence times of intramolecular hydrogen bonded pairs, is comparable to that for the relaxation of the radius of gyration correlation function (see ESI).†

V. Summary/conclusions

In this work we have examined certain static/geometrical properties as well as intra- and intermolecular hydrogen bonding involving characteristic dendrimer sites, in aqueous solutions of G3 and G4 PAMAM dendrimers at different pH conditions, with, or without the presence of linear PEO chains.

In the absence of linear PEO, the degree of deviation of the dendrimers' shape from the spherical geometry in PAMAM/water systems, showed a weak dependence on the

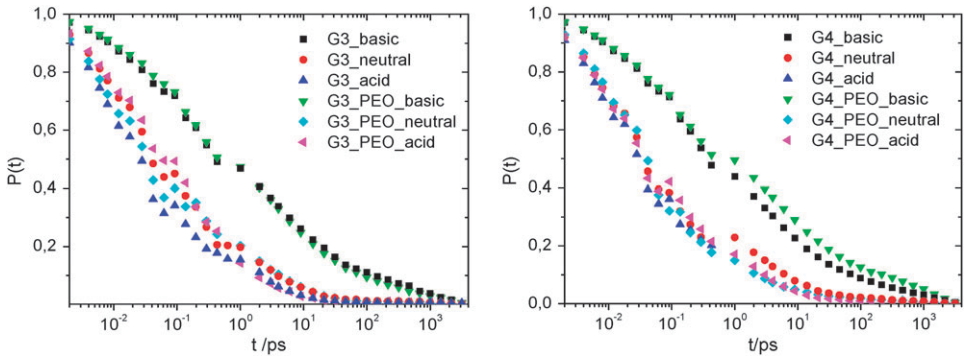

Fig. 9 Hydrogen bonding survival probability function of intramolecular carbonyl oxygen (O)-primary amine hydrogen (H3) pair describing the G3 (left) and the G4 (right) models.

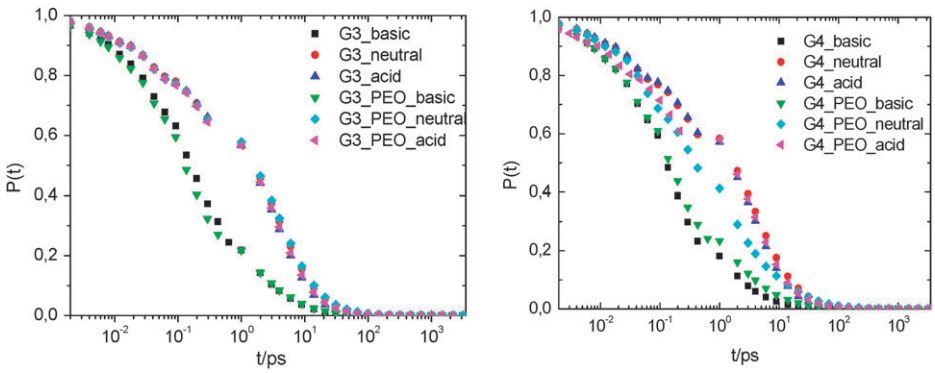

Fig. 10 Hydrogen bonding survival probability functions of intermolecular primary amine hydrogen (H3)–water oxygen (OW) pair corresponding to the G3 (left) and the G4 (right) models.

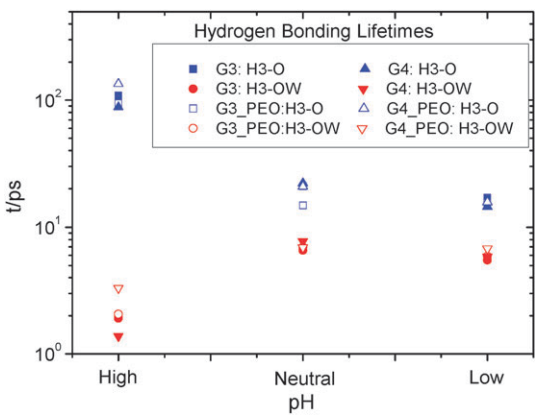

Fig. 11 Liftetimes of the examined intra- (O–H3) and intermolecular (H3–OW) hydrogen bonded pairs. Errors in calculated lifetimes are of the order of 10% or less.

solution's pH in agreement with previous studies.[6] This picture, combined with the significant changes in the density profiles of the dendrimers upon protonation of the primary and tertiary amines, imply that drastic changes in the internal dendritic structure may take place, without necessarily being accompanied by analogous changes in their shape characteristics, in line with recent experimental findings.[5] The presence of the linear PEO polymer close to the PAMAM's periphery increased appreciably the relative shape anisotropy of the dendrimer at physiological pH levels.

Examination of the counterion density profiles indicated that at low pH conditions counterions penetrate well within the dendrimer boundaries in order to neutralize the charged tertiary amines, falling afterwards monotonically toward the dendrimer's periphery. The volume fraction of counterions which penetrated within the dendrimer boundaries exhibited a marked increase between the third (G3) and the fourth (G4) generation dendrimer systems. The changes observed particularly in the G4 density profiles upon protonation, allowed a higher degree of penetration of counterions within the dendrimer interior in agreement with small-angle neutron scattering (SANS) experiments;[65] in these experiments it was observed that the larger relative change in the effective charge upon lowering the pD of the solution (D stands for deuteron), takes place when changing from the third to the fourth generation of PAMAM dendrimers, close to pD $\sim$ 7.

Analysis of the corresponding water profiles with respect to the dendrimer's center of mass, showed that in all cases the density of the solvent remained below the bulk value, thus, providing a new basis for the assessment of relevant experimental observations[10] where this issue was discussed.

While at high pH conditions solvent penetration was rather limited to dendrimer's periphery, in the low pH regime water density profiles remained almost flat at distances away from the core region and the periphery, irrespectively of the dendrimer size. At all pH conditions, the volume fraction of the penetrating water molecules with respect to the volume of the sphere defined by the dendrimer boundary, increased upon

decrease of pH, but did not essentially depend on the dendrimer size in accordance to experimental findings.[10] The effect of the presence of PEO in the aforementioned density profiles was rather weak. Minor changes could only be noted in systems of the 4th generation, probably due to the more open structure assumed by the larger size dendrimers.

The examination for the capability of the studied models for intra- and intermolecular hydrogen bonding, showed that such an association between intra-dendrimer sites and between dendrimer and PEO or water molecules, may play an important role in the ability of these systems to form complexes with hydrogen-bonding-capable substances, as well as in the conformational characteristics of the dendrimer molecules themselves.

Specifically, from the examination of intramolecular hydrogen bonding of the H3–O pairs, it was found that hydrogen bond formation was much more frequent and the formed pairs were much longer-lived at high pH conditions. The timescale of the relevant residence period is comparable to the time for global conformational changes (as probed, for instance, by the fluctuations in the squared radius of gyration, see ESI).† Under these conditions no hydrogen bonding between PEO and dendrimer is detected. Upon protonation, a dramatic drop in intramolecular hydrogen-bond formation is observed. This effect can be rationalized by taking into account that the more open structures assumed by protonated systems, allowed an increased solvent penetration and consequently the formation of "competitive" PAMAM/water hydrogen bonds. The almost 50% lower number of H3–O intramolecular hydrogen bonds in the low pH as compared to the neutral pH systems (Fig. 4), could be ascribed to the combined effect of the increase of the volume fraction of the penetrating solvent molecules and the possibility of hydrogen bond formation between the carbonyl oxygen and the charged tertiary amines. The effects of the dendrimer size and the presence of PEO do not seem to impart noticeable changes to the above picture.

On the other hand, intermolecular hydrogen bonding between PAMAM and water, as well as between PAMAM and PEO, was found to be particularly favored in protonated systems. In the examined H3–OW pair, the average number of hydrogen bonds per H3 sites increased almost by a factor of 6 upon protonation of the amines, while the characteristic residence time was prolonged almost by an order of magnitude in comparison to the non-protonated state. These characteristics do not differentiate substantially between systems of different dendrimer generations, but a decrease of 3 to 5% in the number of formed pairs is observed in the presence of PEO. The latter could be attributed to the antagonistic action of PEO in forming hydrogen bond pairs with the PAMAM H3 sites, as noted earlier. In protonated systems the number of hydrogen bond pairs between PAMAM primary amine hydrogens and PEO ether oxygens, almost doubles at low pH compared to neutral pH conditions. This effect implies that PAMAM/PEO complexes formed at low pH solutions can be expected to be more stable.

In general, concerning the presence of a PEO chain near the PAMAM dendrimers, we can conclude that it only moderately affects the conformational properties of dendrimer, but does play an appreciable role regarding its intra- and intermolecular hydrogen-bonding properties, depending on the solution's pH. It must be noted that the above conclusions were drawn based on the presence of a single PEO chain, which would correspond to experimental conditions in the dilute regime and when a 1 : 1 molar ratio between dendrimer and PEO was examined. Despite these limitations, we expect that features such as the dependence of the degree of hydrogen-bonding between PEO and PAMAM dendrimer as a function of solution's pH, as well as the pertinent residence timescales of the hydrogen bonded pairs, will be also relevant to systems with higher PEO concentrations and/or of different PEO molecular weights.

To conclude, we believe that the above findings regarding the behavior of PAMAM dendrimers in aqueous solutions, with, or without the presence of linear PEO chains, may provide a more detailed basis for the interpretation behavior of water soluble, hydrogen-bonding-capable, hyperbranched-based systems.

Acknowledgements

Funding from the Greek General Secretariat for Research and Technology and the European Community under the framework of the PENED 2003 program (Grant No. 03EΔ716) is gratefully acknowledged. Part of this work was carried out under the HPC – EUROPA project (RII3-CT-2003-506079), with the support of the European Community-Research Infrastructure Action under the FP6 "Structuring the European Research Area" Programme. This study was performed in the framework of the ESF COST action TD0802 "Dendrimers in Biomedical Applications".

References

1 Y. Y. Cheng, Z. H. Xu, M. L. Ma and T. W. Xu, *J. Pharm. Sci.*, 2008, **97**, 123–143.
2 C. Dufes, I. F. Uchegbu and S. A. G., *Adv. Drug Delivery Rev.*, 2005, **57**, 2177–2202.
3 P. Welch and M. Muthukumar, *Macromolecules*, 1998, **31**, 5892–5897.
4 I. Lee, B. D. Athey, A. W. Wetzel, W. Meixner and J. J. R. Baker, *Macromolecules*, 2002, **35**, 4510–4520.
5 W. Chen, D. A. Tomalia and J. L. Thomas, *Macromolecules*, 2000, **33**, 9169–9172.
6 P. K. Maiti, T. Çağin, S.-T. Lin and W. A. Goddard, *Macromolecules*, 2005, **38**, 979–991.
7 W. R. Chen, L. Porcar, Y. Liu, P. D. Butler and L. J. Magid, *Macromolecules*, 2007, **40**, 5887–5898.
8 A. Topp, B. J. Bauer, J. W. Klimash, R. Spindler, D. A. Tomalia and E. J. Amis, *Macromolecules*, 1999, **32**, 7226–7231.
9 A. V. Lyulin, G. R. Davies and D. B. Adolf, *Macromolecules*, 2000, **33**, 6899–6900.
10 T. F. Li, K. Hong, L. Porcar, R. Verduzco, P. D. Butler, G. S. Smith, Y. Liu and W. R. Chen, *Macromolecules*, 2008, **41**, 8916–8920.
11 M. H. Kleinman, J. H. Flory, D. A. Tomalia and N. J. Turro, *J. Phys. Chem. B*, 2000, **104**, 11472–11479.
12 *Dendrimers in Medicine*, ed. B. Klajnert and M. Bryszewska, Nova Science Publishers, 2007.
13 T. Imae and A. Miura, *J. Phys. Chem. B*, 2003, **107**, 8088–8092.
14 V. A. Kabanov, V. G. Sergeyev, O. A. Pyshkina, A. A. Zinchenko, A. B. Zezin, J. G. H. Joosten, J. Brackman and K. Yoshikawa, *Macromolecules*, 2000, **33**, 9587.
15 O. M. Milhem, C. Myles, N. B. McKeown, D. Attwood and A. D'Emanuele, *Int. J. Pharm.*, 2000, **197**, 239–241.

16 U. Gupta, H. B. Agashe, A. Asthana and N. K. Jain, *Biomacromolecules*, 2006, **7**, 649–658.
17 B. Devarakonda, R. A. Hill and M. M. de Villiers, *Int. J. Pharm.*, 2004, **284**, 133–140.
18 L. Fernandez, M. Gonzalez, H. Cerecetto, M. Santo and J. J. Silber, *Supramol. Chem.*, 2006, **18**, 633–643.
19 I. Tanis and K. Karatasos, *J. Phys. Chem. B*, 2009, **113**, 10984–10993.
20 Anna U. Bielinska, Chunling Chen, Jennifer Johnson and J. James R. Baker, *Bioconjugate Chem.*, 1999, **10**, 843–850.
21 H. L. Crampton and E. E. Simanek, *Polym. Int.*, 2007, **56**, 489–496.
22 G. F. Pan, Y. Lemmouchi, E. O. Akala and O. Bakare, *J. Bioact. Compat. Polym.*, 2005, **20**, 113–128.
23 P. K. Maiti and B. Bagchi, *Nano Lett.*, 2006, **6**, 2478–2485.
24 R. Jevprasesphant, J. Penny, R. Jalal, D. Attwood, N. B. McKeown and A. D'Emanuele, *Int. J. Pharm.*, 2003, **252**, 263–266.
25 S. Ulrich, M. Seijo and S. Stoll, *Curr. Opin. Colloid Interface Sci.*, 2006, **11**, 268–272.
26 M. Sugimoto, T. Okagaki, S. Narisawa, Y. Koida and K. Nakajima, *Int. J. Pharm.*, 1998, **160**, 11–19.
27 R. S. Dhanikula and P. Hildgen, *Biomaterials*, 2007, **28**, 3140–3152.
28 T. Chang, K. Pieterse, M. A. C. Broeren, H. Kooijman, A. L. Spek, P. A. I. Hilbers and E. W. Meijer, *Chem.–Eur. J.*, 2007, **13**, 7883–7889.
29 T. Ooya, J. Lee and K. Park, *J. Controlled Release*, 2003, **93**, 121.
30 S. Zimmerman and L. Lawless, *Top. Curr. Chem.*, 2001, **217**, 95–120.
31 U. Boas and P. M. H. Heegaard, *Chem. Soc. Rev.*, 2004, **33**, 43.
32 S. V. Lyulin, I. Vattulainen and A. A. Gurtovenko, *Macromolecules*, 2008, **41**, 4961–4968.
33 S. V. Lyulin, A. A. Darinskii and A. V. Lyulin, *Macromolecules*, 2005, **38**, 3990–3998.
34 S. V. Lyulin, A. V. Lyulin, A. A. Darinskii and I. Emri, *Polymer Science, Ser. A*, 2005, **47**, 1217.
35 S. V. Lyulin, K. Karatasos, A. Darinskii, S. Larin and A. V. Lyulin, *Soft Matter*, 2008, **4**, 453.
36 R. C. van Duijvenbode, M. Borkovec and G. J. M. Koper, *Polymer*, 1998, **39**, 2657–2664.
37 G. D. Smith, D. Bedrov and O. Borodin, *J. Am. Chem. Soc.*, 2000, **122**, 9548.
38 P. K. Maiti, T. Çağin, G. Wang and W. A. Goddard, *Macromolecules*, 2004, **37**, 6236–6254.
39 S. J. Weiner, P. A. Kollman, D. T. Nguyen and D. A. Case, *J. Comput. Chem.*, 1986, **7**, 230–252.
40 J. Wang, R. M. Wolf, J. W. Caldwell, P. A. Kollman and D. A. Case, *J. Comput. Chem.*, 2004, **25**, 1157.
41 S.-T. Lin, P. K. Maiti and W. A. Goddard, *J. Phys. Chem. B*, 2005, **109**, 8663–8672.
42 W. L. Jorgensen, J. Chandrasekhar, J. D. Madura, R. W. Impey and M. Klein, *J. Chem. Phys.*, 1983, **79**, 926.
43 A. A. Gurtovenko, S. V. Lyulin, M. Karttunen and I. Vattulainen, *J. Chem. Phys.*, 2006, **124**, 094904.
44 M. R. P. Paulo and M. B. S. Costa, *Photochem. Photobiol. Sci.*, 2003, **2**, 597–604.
45 M. Majtyka and J. Klos, *Phys. Chem. Chem. Phys.*, 2007, **9**, 2284–2292.
46 K. Karatasos, *Macromolecules*, 2008, **41**, 1025–1033.
47 J. Gasteiger and M. Marsili, *Tetrahedron*, 1980, **36**, 3219–3228.
48 P. Posocco, M. Ferrone, M. Fermeglia and S. Pricl, *Macromolecules*, 2007, **40**, 2257–2266.
49 H. Lee, J. R. Baker and R. G. Larson, *J. Phys. Chem. B*, 2006, **110**, 4014–4019.
50 P. Drabik, A. Liwo, C. Czaplewski and J. Ciarkowski, *Protein Eng., Des. Sel.*, 2001, **14**, 747–752.
51 S. T. Cui, *Phys. Rev. Lett.*, 2007, **98**, 138101.
52 A. Savarino, *Retrovirology*, 2007, **4**, 21.
53 S. Shimamoto, T. Yoshida, T. Inui, K. Gohda, Y. Kobayashi, K. Fujimori, T. Tsurumura, K. Aritake, Y. Urade and T. Ohkubo, *J. Biol. Chem.*, 2007, **282**, 31373–31379.
54 P. Nimmanpipug, V. Lee, J. Chaijaruwanich, S. Prasitwattanaseree and P. Traisathit, in *Bioinformatics Research and Development*, 2007, pp. 119–130.
55 I. Tanis, D. Tragoudaras, K. Karatasos and S. H. Anastasiadis, *J. Phys. Chem. B*, 2009, **113**, 5356–5368.
56 H. Lee, R. M. Venable, J. A. D. MacKerell and R. W. Pastor, *Biophys. J.*, 2008, **95**, 1590–1599.
57 G. D. Smith, D. Bedrov and O. Borodin, *Phys. Rev. Lett.*, 2000, **85**, 5583–5586.
58 G. K. Dalakoglou, K. Karatasos, S. V. Lyulin and A. V. Lyulin, *J. Chem. Phys.*, 2007, **127**, 214903.
59 P. K. Maiti, Y. Y. Li, T. Cagin and W. A. Goddard, *J. Chem. Phys.*, 2009, **130**, 144902.
60 K. Karatasos, D. B. Adolf and G. R. Davies, *J. Chem. Phys.*, 2001, **115**, 5310–5318.
61 J. Rudnick and G. Gaspari, *J. Phys. A: Math. Gen.*, 1986, **19**, L191–L193.
62 S. Rathgeber, M. Monkenbusch, M. Kreitschmann, V. Urban and A. Brulet, *J. Chem. Phys.*, 2002, **117**, 4047–4062.
63 S. Rathgeber, M. Monkenbusch, J. L. Hedrick, M. Trollsas and A. P. Gast, *J. Chem. Phys.*, 2006, **125**, 204908.
64 M. Han, P. Chen and X. Yang, *Polymer*, 2005, **46**, 3481–3488.
65 L. Porcar, Y. Liu, R. Verduzco, K. L. Hong, P. D. Butler, L. J. Magid, G. S. Smith and W. R. Chen, *J. Phys. Chem. B*, 2008, **112**, 14772–14778.
66 H. Zhong, J. F. Wang, X. F. R. Jia, Y. Li, Y. Qin, J. Y. Chen, X. S. Zhao, W. X. Cao, M. Q. Li and Y. Wei, *Macromol. Rapid Commun.*, 2001, **22**, 583–586.
67 M. F. Pan, F. Gao, R. He, D. X. Cui and Y. F. Zhang, *J. Colloid Interface Sci.*, 2006, **297**, 151–156.
68 M. Santo and M. A. Fox, *J. Phys. Org. Chem.*, 1999, **12**, 293–307.
69 E. Chiessi, F. Cavalieri and G. Paradossi, *J. Phys. Chem. B*, 2007, **111**, 2820–2827.
70 G. A. Jeffrey and W. Saenger, *Hydrogen Bonding in Biological Structures*, Springer-Verlag, Berlin, 1991.
71 P. Brocorens, R. Lazzaroni and J.-L. Brédas, *J. Phys. Chem. B*, 2005, **109**, 19897–19907.
72 Y. Tamai, H. Tanaka and K. Nakanishi, *Macromolecules*, 1996, **29**, 6761–6769.
73 K. Bhattacharyya, *Acc. Chem. Res.*, 2003, **36**, 95–101.
74 A. Savelyev and G. A. Papoian, *J. Am. Chem. Soc.*, 2006, **128**, 14506–14518.
75 D. Swiatla-Wojcik, *Chem. Phys.*, 2007, **342**, 260–266.
76 J. Texeira, A. Luzar and S. Longeville, *J. Phys.: Condens. Matter*, 2006, **18**, S2353.
77 K. Karatasos and A. V. Lyulin, *J. Chem. Phys.*, 2006, **125**, 184907.
78 K. X. Moreno and E. E. Simanek, *Macromolecules*, 2008, **41**, 4108–4114.
79 D. A. Markelov, S. V. Lyulin, Y. Y. Gotlib, A. V. Lyulin, V. V. Matveev, E. Lahderanta and A. A. Darinskii, *J. Chem. Phys.*, 2009, **130**, 044907–044909.

